



www.serd.ait.ac.th/eric

Comprehensive Experimental and Theoretical Investigation of Solar Radiation Conditions in Botswana: A Semi-Desert Region

N. Nijegorodov, P.V.C. Luhanga and J.G. King

Department of Physics
University of Botswana
P/Bag 0022
Gaborone
BOTSWANA

ABSTRACT

Solar radiation parameters and mean monthly optimum slopes are studied experimentally and theoretically at 10 different locations of Botswana. It is found that throughout Botswana all mean yearly daily solar radiation components are extremely high. Mean monthly optimum slopes are negative (collector should face North) in June and positive (collector should face South) in December.

It was also observed that the UV-component during the last 8 years has increased by about 5 to 7%. It was also found that the filter used in the instrumentation for UV-radiation measurements is slowly degrading, and hence calibration should be done at least every six months of the year.

Cases of anomalous phenomena when direct normal radiation is increasing greatly (and diffuse radiation decreasing) after solar noon, are observed and discussed. It is also found that when humidity is low and visibility is high, hourly I_g -values recorded with a pyranometer can be less than $(I_{bn} \cos^2 \theta_z + I_d)$ values. This discrepancy, which could be quite common for regions with desert conditions (low humidity and turbidity) is discussed and explained.

1. INTRODUCTION

Botswana is situated in the heart of Southern Africa. It is a land locked country lying between latitudes 17°S and 27°S, and longitudes 20°E and 30°E. Almost 70% of the country is covered with the sands of the Kalahari desert. About 70% of the population is rural, of which a large number live in remote areas, separated and thinly populated, where there is no power from the national grid, no infrastructure, and where petroleum products, or coal cannot be delivered economically (Jain et al., [1]). These areas even lack fuel wood because of the semi-desert conditions. At the same time Botswana has excellent solar conditions where there are on average 320 clear, sunny days per year with an average of 21 MJ m⁻² global insolation per day (Andringa, [2]). Hence it is obvious that all power requirements in rural areas of Botswana can be solved by the use of solar energy devices. However, to design the size and estimate the cost of any particular solar device, or system, for any location, one must know the mean monthly direct normal beam, global and diffuse solar radiation. Unfortunately, until recently, reliable experimental solar radiation data were not available in Botswana.

During the eight years covered in this paper main solar radiation parameters such as daily, hourly, instantaneous direct beam, I_{bn} , diffuse, I_d , global, I_g , and ultraviolet (UV) components have been measured at the University of Botswana, and are currently still being measured. Using the obtained experimental data and their analysis as reference, new analytical models to simulate direct beam, diffuse, global solar radiation components and optimum slopes of a collector have been developed. These models that are based on laws of spectroscopy and thermodynamics have enabled the development of a completely new computer program, which requires only meteorological data: temperature, relative humidity, sunshine-hours, and visibility, as input data. The accuracy of this program is $\sqrt{3} - 5\%$.

The objectives of this study are:

(i) to briefly present, new analytical models to simulate solar radiation components and optimum slopes developed at the University of Botswana, (ii) to analyse experimental data of different solar radiation components obtained in the 8 years (1992-1999) in Botswana, (iii) to discuss peculiarities, discrepancies and anomalous phenomena, (iv) to simulate and to analyse main solar radiation components and optimum slopes for 10 synoptic stations of Botswana.

2. BRIEF THEORY

2.1 A Model to Simulate Direct Beam Radiation, I_{bn}

The atmosphere is a mixture of gases which can be considered as ideal, and hence laws of spectroscopy, kinetic theory and thermodynamics can be used to describe it. According to Bouguer's law, the attenuation of monochromatic light in a gas is described as:

$$I(\nu) = I_o(\nu) \exp(-K_\nu l) \quad (1)$$

where K_ν is the extinction coefficient due to absorption or scattering and l is the thickness of the gas layer.

According to Beer's law: $K_\nu = \gamma_\nu C$, where γ_ν is a constant that depends on the gas and the frequency of the light, and C is the density of the gas in molecules or in moles per unit volume.

Solar radiation is not monochromatic and C of the atmosphere is not constant, that is why, strictly speaking, formula (1) can not be used to describe the attenuation of solar radiation by the atmosphere. But it is not difficult to show that in the case of non-monochromatic light and irregular C , formula (1) can be written as:

$$I = I_o \exp(-\bar{K}n) \quad (2)$$

where n - the total number of molecules in a column of the gas which is given by:

$$n = \int C(x) dx$$

and \bar{K} is the average attenuation coefficient which for a layer of the same thickness can be defined as follows:

$$\bar{K} = -\frac{1}{n} \ln \left(\frac{I}{I_o} \right) \quad (3)$$

The attenuation of solar radiation by the atmosphere is caused by two simultaneous processes:

i) scattering by air molecules and aerosols, and ii) absorption by O_3 , H_2O and CO_2 molecules. Taking into account eqn.(2) the process of attenuation can be expressed as:

$$I_{bn} = I_{on} \exp(-\bar{k}_s N_s - \bar{k}_a N_a - N_o \bar{k}_o - \bar{k}_c N_c - \bar{k}_w N_w) m \quad (4)$$

where N_s , N_a , N_o , N_c , N_w - are values which are proportional to the number of molecules of air, aerosols, ozone, carbon-dioxide, and water vapour in the vertical air column, respectively. If, for example, N_s , N_a , N_o , N_c , and N_w are given in moles, then \bar{k}_s , \bar{k}_a are average molar extinction coefficients due to Rayleigh and turbidity scattering, and \bar{k}_o , \bar{k}_c , \bar{k}_w are average molar extinction coefficients due to absorption by O_3 , CO_2 and H_2O , and m is relative mass. For eqn.(4), I_{bn} can be measured, I_{on} and m can be easily calculated, N_s , N_c and N_w can be calculated by using laws of kinetic theory and thermodynamics, N_o can be estimated (Van Heuklon, [3]), and only N_a is difficult to find. In reference [4] it was shown that equation (4) could be written as:

$$I_{bn} = I_{on} \exp \left(-\bar{k}_s N_s - \frac{\bar{k}_n}{V} - \bar{k}_o N_o - K_c N_c - \bar{k}_w N_w \right) m \quad (5)$$

where V is visibility in km and \bar{k}_s s the modified extinction coefficient due to aerosols.

Now all the atmospheric variables in eqn.(5) can be found, hence, all five extinction coefficients, namely \bar{k}_s , \bar{k}_n , \bar{k}_o , \bar{k}_c , and \bar{k}_w can be obtained by solving five linear equations shown below:

$$\bar{k}_s N_s + \frac{\bar{k}_n}{V} + \bar{k}_o N_o + \bar{k}_c N_c + \bar{k}_w N_w + \frac{1}{m} \ln \left(\frac{I_{bn}}{I_{on}} \right) = 0 \quad (6)$$

where $i = 1, 2, 3, 4$, and 5.

By applying Dalton's law: $P = E_i n_i kT$ and Boltzmann's distribution

$$n = n_o \exp \left(-\frac{mgh}{kT} \right)$$

to the atmosphere, one can derive the following formulae for the variables N_w , N_s and N_c :

$$N_w = \frac{P_w}{M_w g}; N_s = \left(\frac{P - P_w}{M_a g} + \frac{P_w}{M_w g} \right); N_c = \left(\frac{P - P_w}{M_a g} \right) 0.000314 \quad (7)$$

where P and P_w are total air pressure, and partial pressure caused by H_2O , respectively; M_a is average molecular weight of dry air; M_w - molecular weight of water. The derivations of formulae (7) at the procedure of obtaining \bar{k}_s , \bar{k}_n , \bar{k}_o , \bar{k}_c and \bar{k}_w are given in [4].

2.2 A Model to Simulate Diffuse Radiation, I_d

According to reference [5], instantaneous diffuse radiation can be simulated with the help of the following formulae:

$$I_d = I_{on} \frac{K_t e^{-(m-1)K_t}}{e^{K_t} - 1} (0.5K_s + 0.7K_{st} f) \quad (8)$$

$$\frac{I_d}{I_{bn}} = \frac{K_t e^{K_t}}{e^{K_t} - 1} (0.5K_s + 0.7K_{st} f) \quad (9)$$

where I_{on} is direct normal extra-terrestrial radiation; K_t is total attenuation coefficient; K_s is Rayleigh scattering coefficient; K_{st} is turbidity scattering coefficient (if meteorological parameters are known, values of K_s , K_t and K_{st} are found using the parameterization method [5]); and f is an empirical function of zenith angle and air mass.

$$f = f' \left[1 + \frac{0.5K_s}{f_j' K_{st}} \right] - \frac{0.5K_s}{f_j' K_{st}} \quad (10)$$

where

$$f' = \frac{\cos \theta_z}{\frac{2.634}{1 + 1.4196m} - 0.0885} \quad (11)$$

m should be calculated by using the equation given in reference [6]:

$$m = \left[\frac{\sqrt{H(H+2r) + r^2 \cos^2 \theta_z} - r \cos \theta_z}{H} \right] e^{-\left(\frac{MgA}{RT}\right)} \quad (12)$$

where: r - radius of the earth, θ_z - zenith angle, H is the effective thickness of the atmosphere, M is the average molecular weight of air, g is acceleration due to gravity, T is absolute temperature (in K), and A is altitude in metres. Function f is the anisotropic correction factor. At $\theta_z = 0$, $f = 1$ and then it decreases upwards to $\theta_z = 70^\circ$, becoming equal to 1 again at $\theta_z = 90^\circ$.

2.3 An Analytical Model to Simulate Daily Optimum Slope

According to reference [7], a daily optimum slope is obtained by maximizing the daily total insolation received on a tilted surface with respect to the tilt angle, i.e.

$$\frac{d}{d\beta}(H_T) = 0 \quad (13)$$

where

$$H_T = K \frac{12 \times 3600}{\pi} \left[\int_{W_s}^{W_s'} (I_{br} + I_{dr} + I_{rr}) dW \right] \quad (14)$$

where K is constant, W_s' is the sunset hour angle, I_{br} , I_{dr} and I_{rr} are the instantaneous beam, diffuse and ground reflected radiation on a tilted surface. All the necessary details about this method are given in reference [7].

Based on new models to predict direct beam, diffuse, solar radiation and mean daily optimum slopes a new algorithm [8] to simulate all mean monthly solar radiation components and optimum slopes is introduced.

3. EXPERIMENTAL DATA AND INSTRUMENTATION

Daily global insolation on a horizontal surface is recorded continuously at several synoptic stations and at the University of Botswana. Over a number of years, daily total insolation on a tilted surface ($\exists = -30^\circ$) was recorded at the Botswana Technology Centre. Hourly, and instantaneous direct normal, global diffuse and UV-components are continuously recorded at the University of Botswana. All these measurements are done with EPLAB equipment; namely: Normal Incidence Pyrheliometer (Model NIP), Solar tracker (Model ST-3), Precision Spectral Pyranometers (Models PSP), Ultraviolet Radiometers (Models TUVR) with spectral response from 295 to 385nm.

4. ANALYSIS AND DISCUSSION

4.1 Analysis and Discussion of Experimental Results

Analyses show that the instantaneous direct normal radiation at Solar noon can be as high as 1150 W.m^{-2} ; at 30 minutes before sunset it can be 600 W.m^{-2} , and at sunset or sunrise (i.e. half of the solar disc under the horizon), it can be over 100 W.m^{-2} . Examples of hourly solar radiation recorded under different meteorological conditions are given in figure 1. On October 1, 1995, the temperature changed from 20°C in the morning to 32°C at 1700 hours, the pressure was almost constant (910 mb) and relative humidity was around 22 to 26%. Around 0800 hours, a strong wind stirred a large amount of dust thereby making the diurnal profile of I_{bn} completely irregular. On October 2 (the next day), it was still very dusty (visibility less than 15km) but no wind. The temperature, pressure and relative humidity remained

the same. On October 3, the temperature, pressure and relative humidity again did not change significantly. The dust settled down, visibility was above 20 to 25km in the morning and then increased suddenly to 60 to 75km around mid-day.

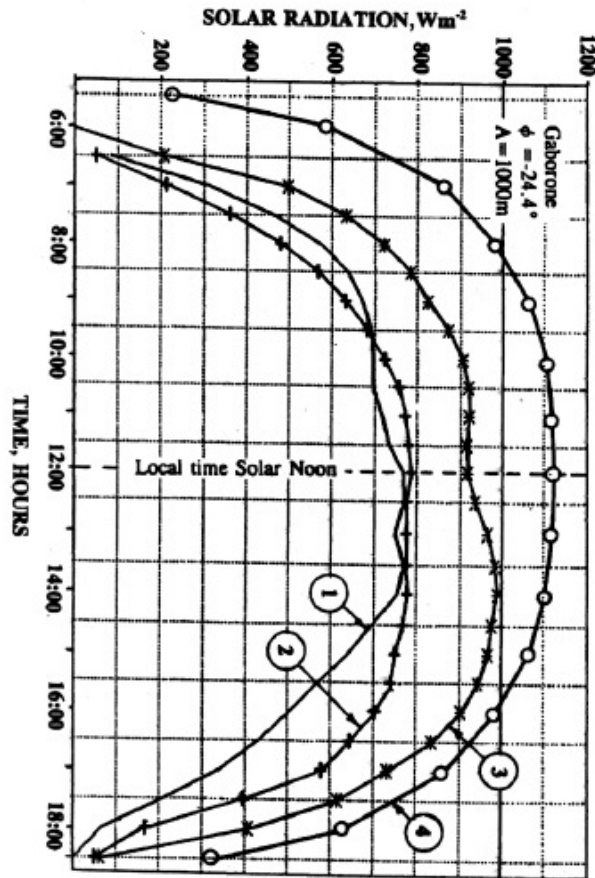


Fig.1. Direct normal solar radiation recorded at University of Botswana. (1) October 1; (2) October 2; (3) October 3; and (4) November 25, 1995.

On November 25 the same year, the sky was extremely clear (visibility was over 70km), I_{bn} at Solar noon was equal to 1120W.m^{-2} , and the diurnal profile was normal with no phase shift. All the instantaneous solar radiation components recorded on October 3 are shown in figure 2. This case is extremely interesting because, in the afternoon, I_{bn} suddenly increased from 920W.m^{-2} at 1200 hours to 990W.m^{-2} at 1400 hours. The only one explanation of this phenomenon could be that at around 1300 hours, a hot wind began to blow from the Kalahari desert and the small water droplets in the air vaporised. It is necessary to note that while I_{bn} was increasing, diffuse components were decreasing so that global radiation did not increase significantly; though it also showed a big phase shift (about 15E). The phase shift of I_{bn} was about 30E. The change in visibility had no effect on the UV component (curve 4) which did not exceed 2.5% of the global radiation. The dashed line (figure 2) shows a qualitative change in visibility. The anomalous phenomenon observed on October 3 could be quite frequent in regions with low humidity and turbidity. This phenomenon was observed several times. It needs further investigation. Analysis of daily insolation on clear, cloudless days (figure 3) showed that the daily direct normal insolation can exceed 45MJ.m^{-2} in December and can be over 30MJ.m^{-2} in June. Mean daily global

insolation varies from $31\text{MJ}\cdot\text{m}^{-2}$ in December to $17\text{MJ}\cdot\text{m}^{-2}$ in June. Such big values of the mean daily insolation can be explained by low humidity and turbidity. Depending on the meteorological conditions, hourly and daily radiation usually varies within 20 to 25%. It is found that the value calculated as $I_{bn} \cos 2_z + I_d$ can be even slightly greater than I_g recorded by a pyranometer if the humidity and turbidity are very low. However, if the humidity is high (greater than 50%) and the visibility is normal ($V = 20\text{-}25\text{ km}$) or less, there is no discrepancy between I_g recorded by a pyranometer and the $(I_{bn} \cos 2_z + I_d)$ value.

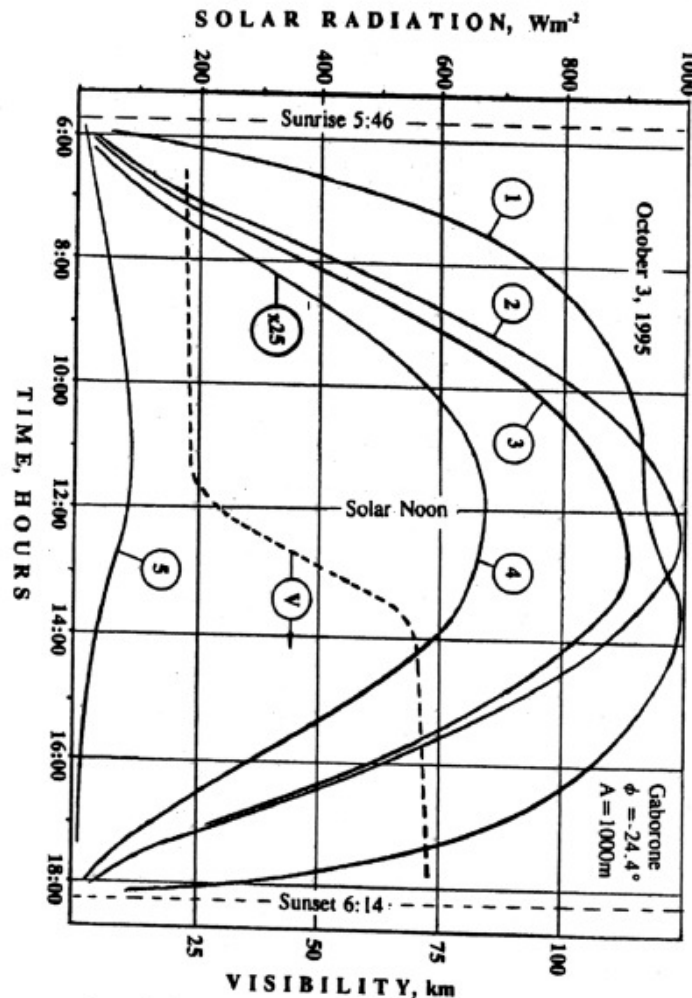


Fig.2. Instantaneous solar radiation components recorded at the University of Botswana on October 3, 1995. (1) Direct normal; (2, 3, 4, and 5) global, beam, UV-component and diffuse radiation on a horizontal surface.

It means that this discrepancy cannot be explained by error in calibrations of the pyranometer and the pyrhemometer. This discrepancy can be explained as follows: when the humidity is low, the absorption of the solar radiation by water vapour is also low and the attenuation factor due to scattering by aerosols decreases significantly (figure 4). Because of the above two reasons, the contribution of the infra-red (IR) part of the solar radiation increases. However, due to the specific geometry of the pyranometer or due to its calibration method, the IR-component is not fully recorded. The discussed discrepancy is very important and needs further investigation.

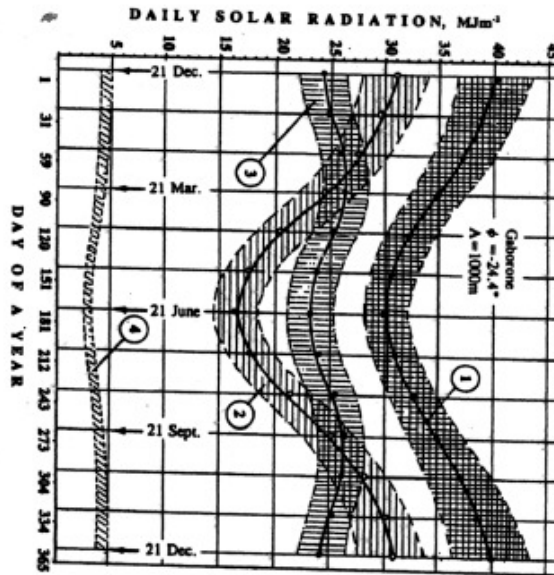


Fig.3. Variation of experimental daily solar radiation components with day of the year for clear, cloudless weather. (1)-direct normal; (2 and 4) global and diffuse on a horizontal surface; (3) total on a tilted surface ($\beta = -30^\circ$).

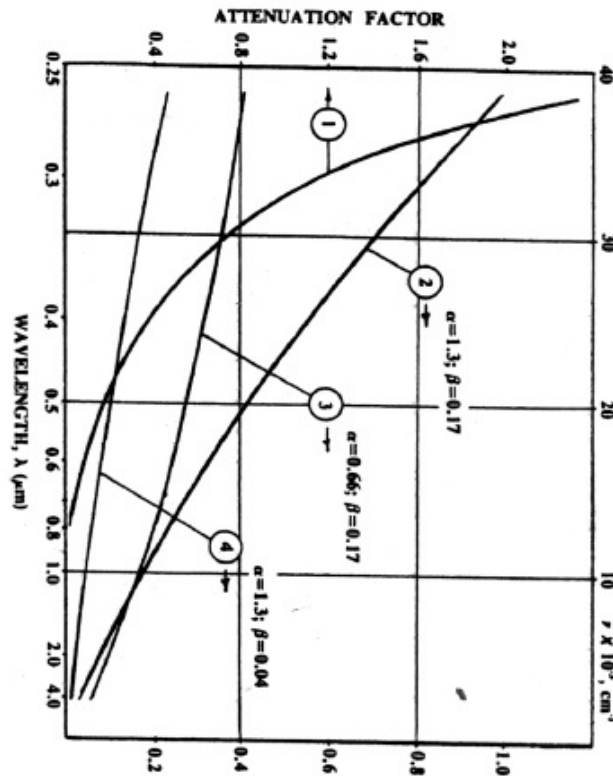


Fig.4. Dependence of attenuation factors upon wavelength. (1) Rayleigh scattering and (2, 3, and 4) atmospheric turbidity. Arrows direct to the corresponding scale.

The UV-component of Solar radiation has been recorded at the University of Botswana (UB) campus since February 1992. The results obtained from the analysis of the data recorded are extremely interesting [9-11]. First of all, it is discovered that the UV-filter of the Ultraviolet Radiometer (EPLAB Model TUVR) is slowly degrading. It is quite evident from figure 5. This tendency to degradation was noticed some time ago; hence a new UV Radiometer of the same type and model was bought to check this. The comparison of the data recorded by the two radiometers allowed us to introduce the correction factor. After correction of the data, the variation of the daily UV-component with the days of the years looks very different see figure 5. The crests of the graphs show the values of the UV in the middle of December and the troughs in the middle of June. The envelopes of the graphs give the variation of the daily UV on clear cloudless days. The scatter or spread of the points (from the envelope) is caused by: clouds (especially in December and January), turbidity of the atmosphere, and dust stirred by windy weather (especially in August, September and October). When it is completely cloudy, the daily UV-radiation drops down to 0.02MJ.m^{-2} or even less. For December, when the sky is clear, the humidity low and visibility high (low turbidity), the daily UV-radiation can be as high as 1.9MJ.m^{-2} . Analysis of figure 5, especially for values of the UV-component at troughs, shows that the daily UV-component during the past 5 years has increased by approximately 7%. Usually the daily UV-component does not exceed 5% of the global radiation. This is also true for the mean year UV-component, which is equal to 4.94% of global. Note that the value of the yearly mean of the UV-component is also increasing. During the 5 years it increased from 4.81% in 1992 to 5.30% in 1996, which gives an over-all increase of 10%. All these observations show that the ozone layer over Botswana is slowly getting depleted.

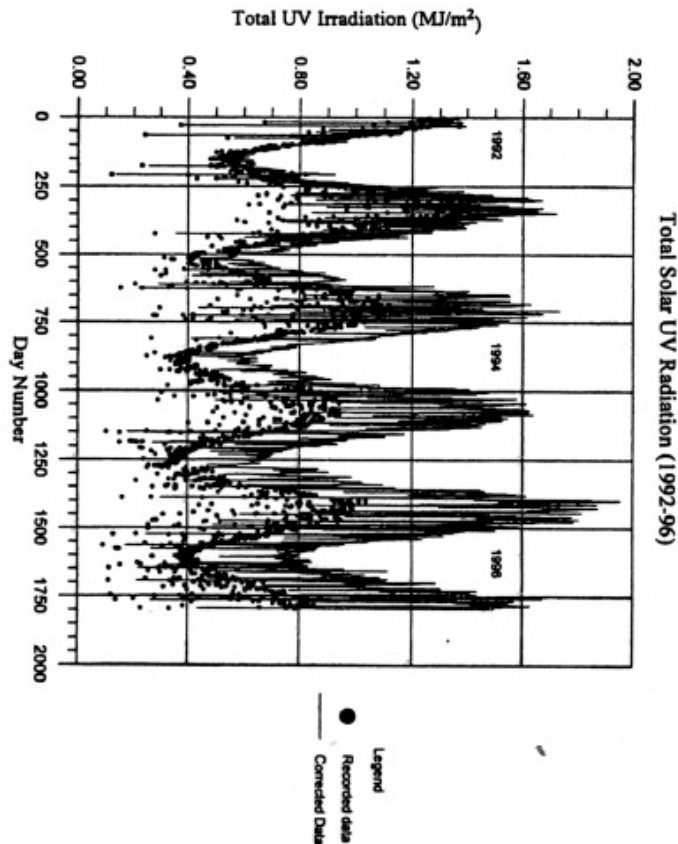


Fig. 5. Variation of the daily UV-component of solar radiation with time; before and after correction.

4.2 Analysis and Discussion of Simulated Results

Solar radiation parameters, optimum slopes (θ_{opt}) and clearness indices (K_t) are simulated for 10 synoptic stations of Botswana. Results of simulation for Gaborone synoptic station (the capital of Botswana) are presented in table 1. Simulated results of mean monthly daily solar radiation parameters and optimum slopes presented in the form of graphs are shown in figure 6. All solar radiation components, clearness indices and optimum slopes are simulated for Julian days, hence the results can be treated as mean monthly solar radiation data. The top part of the table presents the result of simulation for clear, completely cloudless days, and the bottom part shows the results of simulation for partly cloudy weather, i.e. for conditions determined by mean monthly meteorological parameters. In the process of simulation it was assumed that the mean monthly visibility is equal to the standard one (23 km), and the thickness of the ozone layer is also standard (0.34 cm).

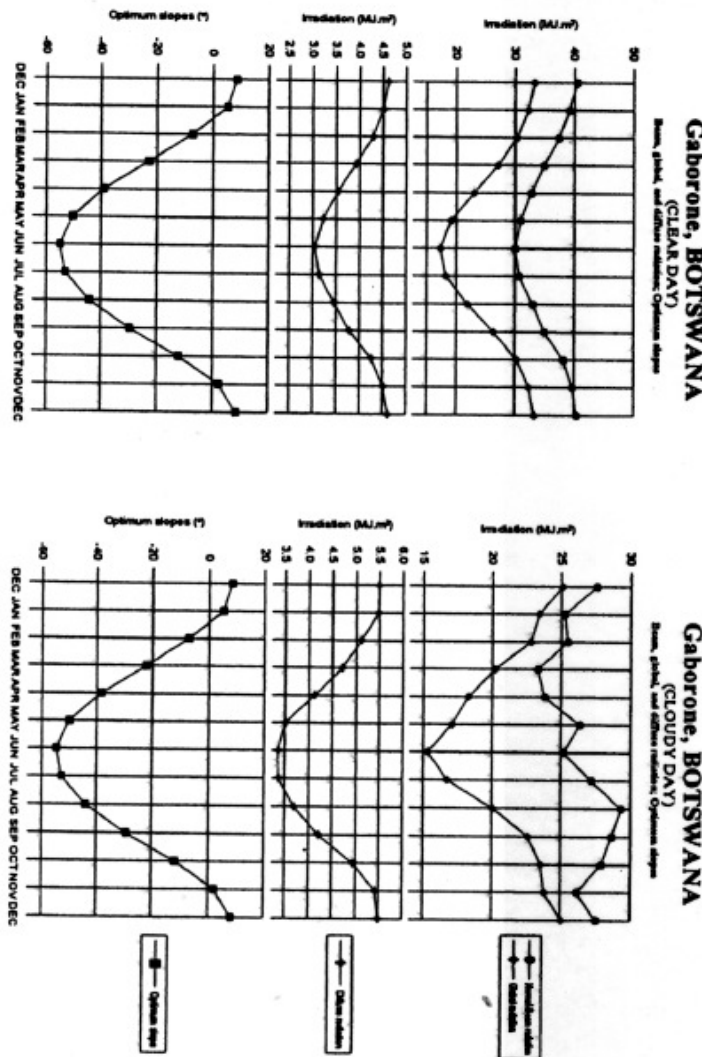


Fig. 6. Variation of daily direct normal, diffuse, and global solar radiation and optimum slope with month of year.

From table 1, one can conclude that all mean year daily solar radiation parameters for Gaborone are extremely high. For partly cloudy weather these parameters are: I_{bn} exceeds $26 \text{ MJ m}^{-2} \text{ day}^{-1}$, H_d is about $4.5 \text{ MJ m}^{-2} \text{ day}^{-1}$, and I_g is $20.75 \text{ MJ m}^{-2} \text{ day}^{-1}$. Optimum slopes for completely clear days and for partly cloudy days are almost the same. Mean monthly optimum slopes vary from -55° in June (collector should face the North) to 9° in December (collector must face South). The mean year optimum slope is approximately -25° . Mean yearly daily results for partly cloudy weather for all 10 synoptic stations and average yearly daily results for the whole of Botswana are shown in table 2. The following are the mean yearly daily solar radiation parameters for Botswana: $H_{bn} = 26.33 \text{ MJ m}^{-2} \text{ day}^{-1}$, $H_d = 4.49 \text{ MJ m}^{-2} \text{ day}^{-1}$, $H_g = 21.06 \text{ MJ m}^{-2} \text{ day}^{-1}$. The mean year optimum slope for Botswana is -22° (collector should face North). But we observe that at present all commercial solar panels are installed at -30° ; which is wrong.

It is also necessary to mention that if the slope of a solar panel could be adjusted at least once a month, the efficiency of the PV-arrays could be boosted by 15 - 20% at almost no additional investment. High values of mean yearly daily solar radiation parameters for Botswana can be explained by the high sunshine hours (almost 9 hours per day throughout Botswana) and by the low humidity.

Table 1. Simulated Mean Monthly Daily Solar Radiation Parameters, Clearness Indices and Optimum Slopes for Gaborone

GABORONE - BOTSWANA: Alt:983m, Lat: 24°40S, L= -24.87°, Long: 25°55E								
CLEAR WEATHER								
	Jul. Day	Hbn	Hd	Hg	Hb(Calc.)	Kt	δ - Opt	
		(MJ/m ² day)	(MJ/m ² day)	(MJ/m ² day)	(MJ/m ² day)		(Degrees)	
1	JAN	17	39.15	4.51	32.33	27.82	0.757	5.20
2	FEB	17	37.41	4.29	30.31	26.02	0.759	-7.49
3	MAR	18	34.96	3.92	27.12	23.20	0.761	-22.88
4	APR	15	32.76	3.54	23.00	19.46	0.775	-39.17
5	MAY	15	30.92	3.22	19.13	15.91	0.786	-50.36
6	JUN	11	30.00	3.05	17.31	14.26	0.795	-54.99
7	JUL	17	30.75	3.14	18.26	15.12	0.801	-53.00
8	AUG	18	33.07	3.46	21.89	18.43	0.806	-44.25
9	SEP	15	35.04	3.79	26.37	22.58	0.798	-29.57
10	OCT	15	36.19	4.26	30.30	26.04	0.790	-12.14
11	NOV	14	39.70	4.51	32.47	27.96	0.776	2.16
12	DEC	10	40.44	4.61	33.33	28.72	0.772	8.40
	Avg.		35.20	3.86	25.99	22.13	0.781	-24.84
PARTLY CLOUDY WEATHER								
	Jul. Day	Hbn	Hd	Hg	Hb(Calc.)	Kt	δ - Opt	
		(MJ/m ² day)	(MJ/m ² day)	(MJ/m ² day)	(MJ/m ² day)		(Degrees)	
1	JAN	17	25.22	5.48	23.40	17.92	0.548	5.02
2	FEB	17	25.45	5.11	22.82	17.71	0.571	-7.27
3	MAR	18	23.31	4.71	20.18	15.47	0.566	-22.23
4	APR	15	23.82	4.12	18.26	14.14	0.616	-38.45
5	MAY	15	26.34	3.50	17.06	13.56	0.701	-50.00
6	JUN	11	25.15	3.35	15.30	11.95	0.703	-54.60
7	JUL	17	27.18	3.36	16.72	13.36	0.733	-52.73
8	AUG	18	29.34	3.69	20.05	16.36	0.738	-43.99
9	SEP	15	28.65	4.21	22.67	18.46	0.686	-29.22
10	OCT	15	27.90	4.95	23.57	18.62	0.625	-11.88
11	NOV	14	26.15	5.43	23.85	16.42	0.570	2.10
12	DEC	10	27.55	5.49	25.06	19.57	0.581	8.16
	Avg.		26.34	4.45	20.75	16.30	0.637	-24.59

Table 2. Simulated mean yearly daily Solar radiation parameters, clearness indices, Optimum slopes for 10 synoptic stations of Botswana

No.	Synoptic Station	Partly cloudy Weather					α_{opt} (degrees)	Sunshine hours
		Hbn (MJ/m ²)	Hd (MJ/m ²)	Hb (MJ/m ²)	Hg (MJ/m ²)	Kt		
1	Francistown	25.62	4.53	16.23	20.76	0.623	-21.4	8.74
2	Gaborone	26.34	4.45	16.30	20.75	0.637	-24.8	8.98
3	Ghanzi	27.40	4.47	17.27	21.74	0.653	-21.9	9.19
4	Kasane	24.39	4.68	15.71	20.39	0.601	-17.7	8.20
5	Mahalapye	24.83	4.55	15.53	20.09	0.610	-23.3	8.48
6	Maun	26.19	4.51	16.67	21.18	0.631	-20.2	8.92
7	Sebele	26.54	4.40	16.50	20.90	0.639	-24.8	9.12
8	Shakawe	24.99	4.57	16.10	20.68	0.611	-18.6	8.55
9	Tsabong	28.92	4.33	17.87	22.20	0.679	-26.2	9.70
10	Tshane	28.05	4.41	17.46	21.87	0.664	-24.2	9.38
	Average	26.33	4.49	16.56	21.06	0.635	-22.3	8.93

5. CONCLUSIONS

The investigations carried out here showed that measurements of solar radiation components in countries with low humidity and low turbidity, like Botswana, have some specific peculiarities, which have to be taken into account. The discrepancy between the I_g -values recorded with a pyranometer and the value of I_g calculated with the formula: ($I_g = I_{bn} \cos^2 \alpha_z + I_d$), obtained with the help of a pyrheliometer and a pyranometer with a shadow-ring, could be very common for countries with desert and semi-desert climates. The degradation of UV-filters of the UV-Radiometer (Model TUVR), which is actually exponential, should also be considered. The rate of degradation depends on the intensity of the UV-radiation, and correction factors could be different for different locations.

Experimental and simulated results show that Botswana is an ideal country to utilize solar energy, using such sophisticated devices as medium-temperature Rankine cycle and high-temperature Rankine cycle (the central tower concept).

6. REFERENCES

- [1] Jain, P.K., Nijegorodov, N., and Kartha, C.G.; Role of Solar Energy in development in Botswana. *Renewable Energy*, Vol.4, No.2, pp.179-188, 1994.
- [2] Andringa, J.; Some characteristics of the pattern of solar radiation in Botswana. *RERIC International Energy Journal*, Vol.11, No.2, pp.69-78, 1989.
- [3] T.K. Van Heuklon, Estimating atmospheric ozone for solar radiation models. *Solar Energy*, 22, 63-68. (1979).
- [4] N. Nijegorodov and P.V.C. Luhanga, A new model to predict normal instantaneous solar radiation, based on laws of spectroscopy, kinetic theory and thermodynamics. *Renewable Energy*, vol. 13, No. 4, pp. 523-530, 1998.
- [5] N. Nijegorodov, J.A. Adedoyin, and K.R.S. Devan, A new analytical-empirical model for the instantaneous diffuse radiation and experimental investigation of its validity. *Renewable Energy*, vol. 11, No.3, pp. 341-350, 1997.
- [6] N. Nijegorodov, and P.V.C. Luhanga, Air mass: analytical and empirical treatment; an improved formula for air mass. *Renewable Energy*, 7(1), 57-65 (1996).
- [7] N. Nijegorodov, K.R.S. Devan, P.K. Jain and S. Carlson, Atmospheric transmission models and an analytical method to predict the optimum slope of an absorber plate, variously oriented at any location *Renewable Energy*, vol. 4, No. 5, pp. 529-543, 1994.

- [8]. N. Nijegorodov, A new algorithm to simulate instantaneous hourly, daily, mean monthly solar radiation parameters and optimum slopes of a variously oriented collector. Proc. of the 4th International Conference on New Energy Systems and Conversions, pp. 209-214, June 27-30, Japan, 1999.
- [9]. P.V.C. Luhanga and N. Nijegorodov; Investigation of solar radiation in Botswana and some anomalous phenomena observed. *Renewable Energy*, 12(4), 401-408 (1997).
- [10]. P.V.C. Luhanga and R.O. Ocaya, Some Characteristics of Solar Ultraviolet Radiometers. *International Energy Journal*, 1(1), 39-44 (2000).
- [11]. P.V.C. Luhanga, Long-term Performance Characteristics of Commercial Solar UV Radiometers. Proc. Of The Regional Conference on Materials Science, Makerere University, Kampala, Uganda. Pp. 155-161, September 1999.